On the influence of structural flexibility on feedback control system stability for EMS Maglev vehicles

T. E. Alberts & G. Oleszczuk
Aerspace Engineering Department, Old Dominion University, Norfolk Virginia, USA

ABSTRACT: This paper presents analysis of stability requirements for EMS magnetically levitated vehicles with structural flexibility taken into account. The implications of collocated versus non-collocated control are contrasted in the context of the stability of flexible modes. A series of simple analytical examples, beginning with a rigid mass and progressing to simplified multi-mode flexible structures are evaluated analytically. The basic guidelines for stability presented are considered extendable to complex maglev systems which have any structural flexibility in their vehicle and guideway structures. Illustrative analytical and experimental laboratory results are presented.

1 INTRODUCTION

1.1 Problem Description

EMS maglev systems can exhibit closed-loop instability due to structural flexibility. In this paper simple structural models are used to explore the impact of flexibility on stability when simple dissipative, decentralized compensators are used.

2 ELECTROMAGNETIC MODEL

2.1 Fundamental modeling

The electromagnetic model employed corresponds to a U-shaped magnet interacting with a U-shaped rail as illustrated in Figure 1.

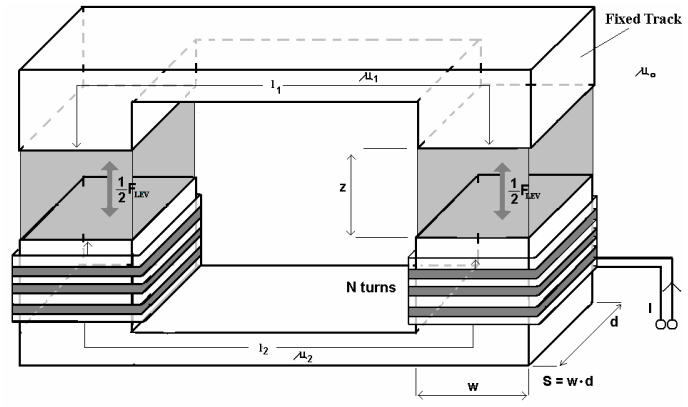

Figure 1: U-Shaped Magnet and Rail

For such a configuration, the electromagnetic force of attraction can be expressed as (Limbert et al. 1976):

$$F = \frac{1}{4}\frac{\mu_0 N^2 I^2 dw}{z^2}\left\{1+\frac{2z}{\pi \cdot w}\right\} \tag{1}$$

In this expression, which was simplified due to assuming zero lateral offset, the symbols μ_0, d, N, w represent respectively permeability, coil length, number of turns, and width of the coil and variables z, and I represent air gap and current. The inductance of the magnet is expressed as:

$$L(z) = \mu_0 dN^2\left[-\frac{w}{2z}-\frac{1}{\pi}\ln\left(\frac{1}{z}\right)\right] \tag{2}$$

2.2 Linearization

For further analysis, the force expression can be linearized (Sinha 1986) with respect to reference values for gap z_0 and current I_0, using the first derivative components from the Taylor series expansion:

$$F \cong F\Big|_{\substack{z_0\\I_0}} \frac{\partial F_{LEV}}{\partial z}\Big|_{\substack{z_0\\I_0}} (z-z_0) + \frac{\partial F_{LEV}}{\partial I}\Big|_{\substack{z_0\\I_0}} (I-I_0) \tag{3}$$

Thus a linear expression for the electromagnetic force is as follows:

$$F \cong k_z z - k_i I \tag{4}$$

where:

$$k_i = \frac{1}{2}\frac{\mu_0 N^2 dw I_0}{{z_0}^2}\left(1+2\frac{z_0}{\pi \cdot w}\right) \tag{5}$$

$$k_z = \frac{1}{2}\frac{\mu_0 N^2 dw {I_0}^2}{{z_0}^3}\left(1+2\frac{z_0}{\pi \cdot w}\right) - \frac{\mu_0 N^2 d {I_0}^2}{2\pi \cdot {z_0}^2} \tag{6}$$

Electromagnets are typically driven by current amplifiers intended to follow a current command I^{Cmd}. A simplified block diagram representing such an arrangement is illustrated in Figure 2, where K_a is a current feedback gain, R is the resistance of the magnet coils, and L is the coil inductance defined previously, linearized about the operating point z_0.

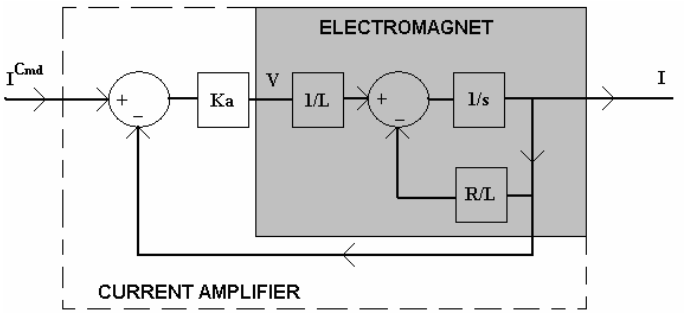

Figure 2: Electrical Model Schematic

The combination of the electrical and electromagnetic components, once linearized, would typically lead to a system such as the one illustrated Figure 3 (Goodall 1985), which represents a single rigid mass being levitated.

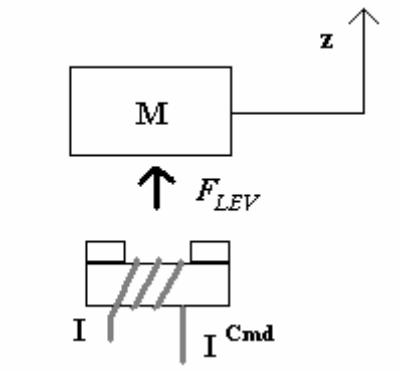

Figure 4: Single Rigid Mass Model

3 ELECTROMECAHNICAL SYSTEMS

3.1 Maglev as a rigid mass

Consider a simple one-degree-of-freedom rigid model of the maglev system (Fig. 4). Equations of motion for the system based on Figures 3 and 4 can be expressed as:

$$\frac{d^2 z}{dt^2} = \frac{k_z}{M} z - \frac{k_i}{M} I \tag{7}$$

Using the standard state-space (Friedland 1986) form (8), the equations of motion for the rigid system are expressed as shown in Equations 9 and 10.

$$\begin{aligned} \dot{\vec{x}} &= A \cdot \vec{x} + B \cdot \vec{u} \\ \vec{y} &= C \cdot \vec{x} + D \cdot \vec{u} \end{aligned} \tag{8}$$

$$\begin{bmatrix} \dot{z} \\ \ddot{z} \\ \dot{I} \end{bmatrix} = \begin{bmatrix} 0 & 1 & 0 \\ \frac{k_z}{M} & 0 & -\frac{k_i}{M} \\ 0 & \frac{k_z}{k_i} & -\frac{(K_a + R)}{L} \end{bmatrix} \begin{bmatrix} z \\ \dot{z} \\ I \end{bmatrix} + \begin{bmatrix} 0 \\ 0 \\ \frac{K_a}{L} \end{bmatrix} I^{Cmd} \tag{9}$$

$$[z] = \begin{bmatrix} 1 & 0 & 0 \end{bmatrix} \begin{bmatrix} z \\ \dot{z} \\ I \end{bmatrix} \tag{10}$$

Based on (9) and (10) the transfer function can be calculated:

$$G_R(s) = \frac{-K_x}{(s-p)(s+p)(s+\alpha)} \tag{11}$$

where:

$$p \cong \sqrt{\frac{k_z}{M}}, \quad \alpha = \frac{K_a + R}{L}, \quad K_x = K_a \frac{k_i}{L} \tag{12}$$

The system has three real poles. One is positive, which is indicative of the inherent instability of the attractive types of Maglev systems. The pole α is associated with current feedback. The real pair $\pm p$ replaces the rigid body poles of the purely structural

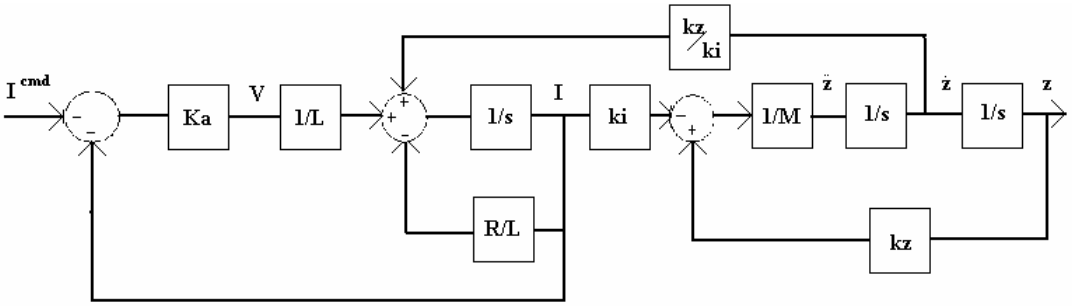

Figure 3: Electromechanical Block Diagram for Magnetically Suspended Rigid Mass

model. The value of p can vary significantly with gap and current.

It is a simple matter to show that the stabilization of this structure can be accomplished using a PD compensator with positive gap feedback. Let the compensator have the form:

$$C_0(s) = K_p + K_D s \tag{11}$$

The feedback structure considered is as shown in Figure 5, where negative feedback is initially assumed.

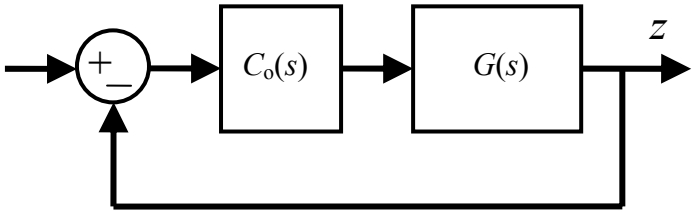

Figure 5: Basic Feedback Structure

The PD compensator is an example of a dissipative controller (Joshi 1989). When used in a simple feedback loop for a single magnet to control the variation of its own air gap, then it is called decentralized (West-Vukovich & Davidson 1984).

Based on the considerations above, the closed-loop transfer function for the rigid single mass system under PD control is:

$$G_R^{CL}(s) = \frac{-K_x(K_P + K_D s)}{s^3 + s^2\ \alpha - s(p^2 + K_x K_D) - (p^2\alpha + K_x K_P)} \tag{12}$$

The *CL* superscript designates closed-loop. The sufficient conditions for the stability of this system are determined using the Routh criterion (Ogata 1970), which produces the following conditions:

$$K_P < \frac{-p^2\ \alpha}{K_x}, \qquad K_D < \frac{-p^2}{K_x}, \qquad K_P > K_D\alpha \tag{13}$$

These conditions indicate the necessity for strictly negative gains K_P and K_D, in other words positive feedback, and moreover, that the gains have a minimum threshold magnitude for stability.

3.2 Maglev as a simple flexible system

As a first step toward evaluation of the impact of structural flexibility on control of a Maglev system, a single flexible mode of the vehicle is introduced through. The new structural model is shown schematically in Figure 6.

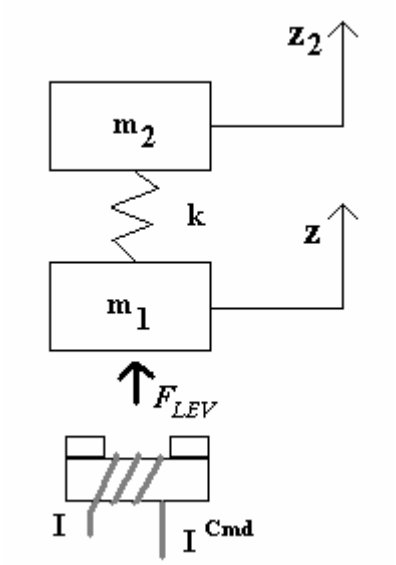

Figure 6: Simple Flexible Structure Maglev System

In this system $m_1 + m_2 = M$ still represents the overall weight of the initial system. The actuator model equation remains the same. The spring constant k represents the flexibility of the vehicle. The displacement resulting from structural flexibility is denoted by z_2, while the electromagnetic air gap is denoted by z. The new equations of motion become:

$$\frac{d^2 z}{dt^2} = \frac{k_z - k}{m_1} z + \frac{k}{m_1} z_2 - \frac{k_i}{m_1} I \tag{14}$$

$$\frac{d^2 z_2}{dt^2} = \frac{k}{m_2} z - \frac{k}{m_2} z_2 \tag{15}$$

$$\frac{dI}{dt} = \frac{\left(I^{Cmd} - I\right)K_a}{L} \tag{16}$$

Similar to the notation of the rigid case, the following notation is introduced:

$$\omega_1^2 = \frac{k}{m_1}, \qquad \omega_2^2 = \frac{k}{m_2}, \qquad p_z^2 = \frac{k_z}{m_1} \tag{17}$$

In state equation associated with these equations can be expressed as:

$$\begin{bmatrix} \dot{z} \\ \dot{z}_2 \\ \ddot{z} \\ \ddot{z}_2 \\ \dot{I} \end{bmatrix} = \begin{bmatrix} 0 & 0 & 1 & 0 & 0 \\ 0 & 0 & 0 & 1 & 0 \\ p_z^2 - \omega_1^2 & \omega_1^2 & 0 & 0 & -K_x \dfrac{L}{K_a} \\ \omega_2^2 & -\omega_2^2 & 0 & 0 & 0 \\ 0 & 0 & 0 & 0 & -\alpha \end{bmatrix} \begin{bmatrix} z \\ z_2 \\ \dot{z} \\ \dot{z}_2 \\ \dot{I} \end{bmatrix} + \begin{bmatrix} 0 \\ 0 \\ 0 \\ 0 \\ \dfrac{K_a}{L} \end{bmatrix} I^{Cmd} \tag{18}$$

The C matrix of the state-space representation (8) depends upon the sensor locations. When the actuator and sensor pairs are located together, the pair is said to be collocated (Joshi 1989). With regard to the present system, the collocated case has C matrix:

$$C_c = [1 \quad 0 \quad 0 \quad 0 \quad 0] \tag{19}$$

The so-called non-collocated[1] case, in which the input is applied to mass 1 and the output is measured from mass 2 has:

$$C_n = [0 \quad 1 \quad 0 \quad 0 \quad 0] \tag{20}$$

The D matrix is zero for either case. Applying the standard transformation from state-space to transfer function form, the open-loop transfer function for collocated plant is:

$$G_c(s) = \frac{-K_x\left(s^2 + \omega_2^2\right)}{s^5 + s^4 a_4 + s^3 a_3 + s^2 a_2 + s a_1 + a_0} \tag{21}$$

in which the denominator coefficients are as follows:

$$a_0 = -p_z^2 \omega_2^2 \alpha, \quad a_1 = -p_z^2 \omega_2^2, \quad a_2 = \alpha\left(\omega_1^2 + \omega_2^2 - p_z^2\right)$$
$$a_3 = \omega_1^2 + \omega_2^2 - p_z^2, \quad a_4 = \alpha$$

The open-loop transfer function for non-collocated plant is:

$$G_n(s) = \frac{-K_x \omega_2^2}{s^5 + s^4 a_4 + s^3 a_3 + s^2 a_2 + s a_1 + a_0} \tag{22}$$

As in the rigid case, it is observed that these transfer functions are unstable and non-minimum phase. For the non-collocated case there are no zeros, a condition that makes the system more difficult to stabilize because it has lower relative degree.

Considering each of these systems in a feedback loop such as Figure 5, and performing a similar Routh analysis, one can evaluate and compare the stability conditions.

3.3 PD Control of the Collocated Flexible System

Routh array analysis of the closed-loop collocated system yields the following conditions for stability:

$$K_P < \frac{-p_z^{\,2}\,\alpha}{K_x}, \qquad K_D < \frac{-p_z^{\,2}}{K_x}, \qquad K_P > K_D \alpha \tag{23a}$$

$$K_P < \alpha \frac{\left(-p_z^{\,2} + \omega_1^2 + \omega_2^2\right)}{K_x} \tag{23b}$$

$$K_D < \frac{\left(-p_z^{\,2} + \omega_1^2 + \omega_2^2\right)}{K_x} \tag{23c}$$

Conditions (23b) and (23c) can be neglected since they are dominated by (23a). Note the similarity of conditions (23a) to conditions (13) for the rigid case, the difference being the replacement of p by p_z in the flexible system. Note also that $p^2 < p_z^2$ because $M > m_1$, therefore:

$$K_P < \frac{-p^2\,\alpha}{K_x} < \frac{-p_z^{\,2}\,\alpha}{K_x} \tag{24}$$

$$K_D < \frac{-p^2}{K_x} < \frac{-p_z^{\,2}}{K_x} \tag{25}$$

Thus it can be concluded that the same strategy that worked to stabilize the rigid system, will always work on the flexible system, however the range of stable gains is more restrictive. In other words, the compensator that stabilizes the flexible system will always stabilize the rigid system, but the reverse is not true. To stabilize the flexible system, the gains that stabilized the rigid system must be scaled up in magnitude by a factor of at least p_z^2 / p^2.

The root locus diagram of Figure 7 illustrates the stabilization of the collocated system using PD control. The arrows indicate the effect of increasing K_D. The zero corresponding to the critical value of K_D (25) is marked 1x while the zero positions for 10 and 100 times the critical value are respectively marked 10x and 100x..

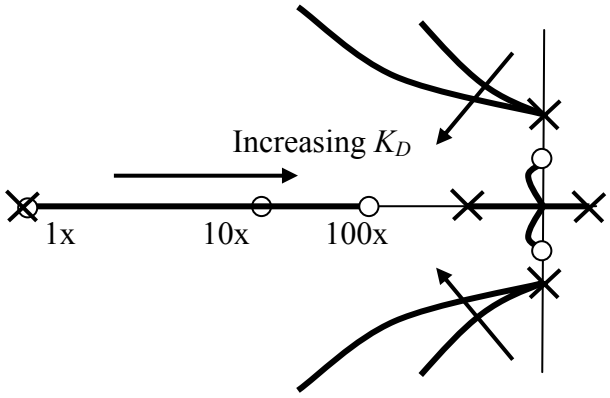

Figure 7: Root Locus of the PD Controlled Collocated System

3.4 PD Control of the Non-Collocated System

If one evaluates the denominator of the collocated system's closed-loop transfer function (not explicitly shown here), it is found that in contrast to the collocated case, only the zero degree and first degree terms are influenced by the controller. Moreover, unlike in to the collocated case, a necessary condition for stability is that:

$$\omega_1^2 + \omega_2^2 > p_z^2 \quad \Rightarrow \quad k\left(1 + \frac{m_1}{m_2}\right) > k_z \tag{26}$$

which is usually satisfied in practice. More critically, the s^3 term in the first column of the Routh table is zero, indicating that the system can be margin-

[1] Since the system considered has only 2 masses, this is an extreme example of non-collocation. Actual system with approximate collocation may be more forgiving

ally stable at best under PD control[2], thus a PD compensator is unable to stabilize the system. Interestingly, the remaining terms indicate that the requirements for marginal stability are the same as the stability requirements (23a) for the collocated case.

4 EXPERIMENTS

4.1 Single DOF Test Rig

A single degree of freedom test rig was constructed using one magnet and a short section of rail from the Old Dominion University Maglev system (Davey et al. 2001). The magnet is capable of producing about 6000 lbs of lift force. The magnet is fixed in place and a section of track is suspended overhead from a lever arm, via a 4-bar linkage that allows vertical movement of the track, but keeps it aligned with the magnet. Weights are hung from the far end of the lever arm with a 4 to 1 mechanical "disadvantage," such that the magnet(s) have to produce 4,000 pounds of attractive force to lift 1,000 pounds for example. The rig is fitted with load cells to measure vertical and lateral load. The lever arm can be locked in place using screw jacks to permit static testing of the magnets, for example to verify magnet force plots. An eddy current based sensor is used for gap measurement.

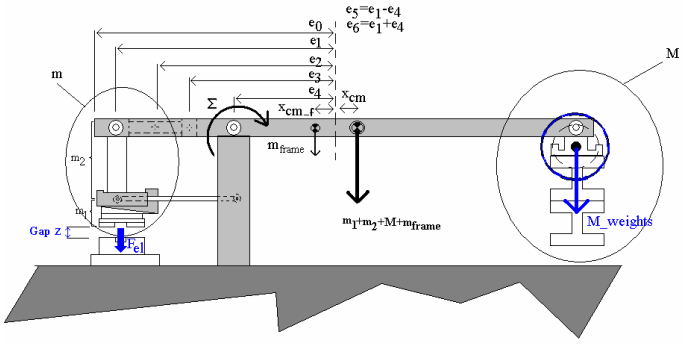

Figure 8: Simple Schematic of the Maglev Test Rig

The test rig was designed to exhibit structural flexibility representative of a full scale system. For lumped parameter analysis, a simplified representation of the system's flexibility was considered, as illustrated in Figure 9. In effect, this model simplifies the structure to three point masses connected by two discrete springs as illustrated in Figure 10.

Bode plots for a collocated (based on mass 1) and non-collocated (output at mass 2) model of the system are given in Figure 11. It can be seen that the non-colocated case is similar to collocated, with the exception that the pair of zeros at 80Hz is not present in the non-collocated case. This is similar to the simple two mass example presented earlier. Note that this plot represents the "levitated" case, that is, when the entire system is floating in space.

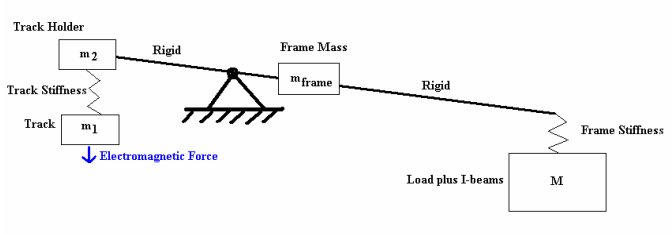

Figure 9: Lumped Parameter Representation of the Test Rig

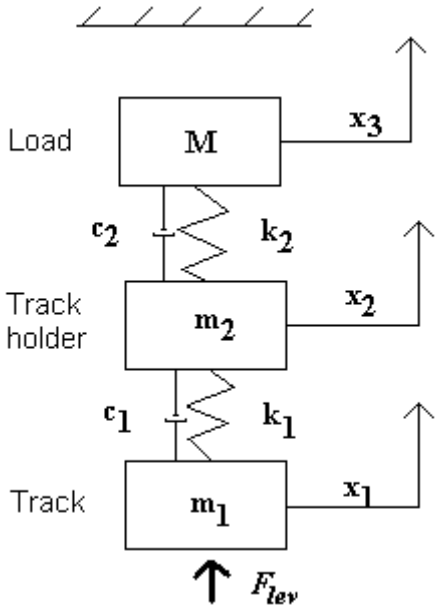

Figure 10: Three Mass Model of the Test Rig

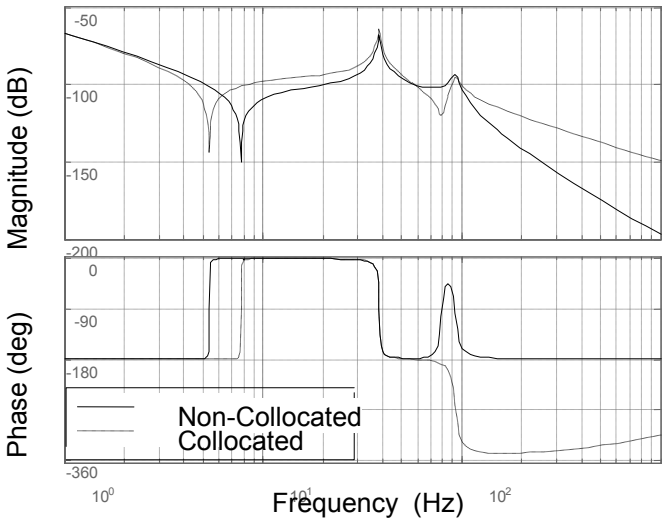

Figure 11: Analytical Bode Plots for the Levitated Test Rig

In practice, it was not practical to experimentally validate the model represented in Figure 10. Instead, the open-loop model of the non-levitated case was verified. This corresponds to the load M resting on the ground, in effect locking it in place which would be equivalent to setting x_3 to zero.

A Hewlett Packard dynamic signal analyzer was used to verify this case using 3 different air gap settings. The test was performed by driving the magnet current with a sine sweep input while monitoring the

[2] Not necessarily the case in actual system with non-zero damping and with approximate collocation

air gap reading. The analytical and experimental results were found to be in close agreement.

4.2 Levitation Control of the Test Rig

Numerous successful levitation experiments have been conducted using the ODU single degree of freedom test rig. Controllers are implemented using a Matlab® application known as xPC Target®. With this application, a compensator constructed graphically using Matlab's Simulink® environment on a host computer, can be converted to C-code and compiled, then uploaded to the target machine. In this particular test configuration a desktop PC computer was used as a host. A PC104 single based computer with Intel 468 series processor was used as a target. Communication between these two devices was established via Ethernet. The PC104 computer was equipped with a PCI based National Instruments data acquisition card. The sample rate for was set to 20 kHz. The high sample rate was used to allow over-sampling of the measurements so that digital filters could be used to help reduce signal noise.

Typically, to obtain acceptably stable results, controller designs had to be slightly more conservative in terms of gain and phase margin than analysis suggested. It is believed that this was primarily due to the following factors:

- Discrete time implementation
- The use of anti-aliasing filters
- Model uncertainty
- Electromagnetic non-linearities

The use of gap feedback with PD or similar controllers was found to be undesirable because of the tendency of the derivative term to amplify measurement noise. To avoid this problem, the scheme of combining the derivative of a low-pass filtered gap measurement with the integral of high-pass filtered (actually a "leaky" integrator) acceleration signals was very effective. In the interest of brevity, the experimental implementation is not exhaustively covered here; however a typical result is presented in Figure 12. The controller was designed as a PD controller, based on the principles described in this paper. After suitable performance was achieved, an error integrator term was added to reduce steady state error. The commanded gap value was 0.4".

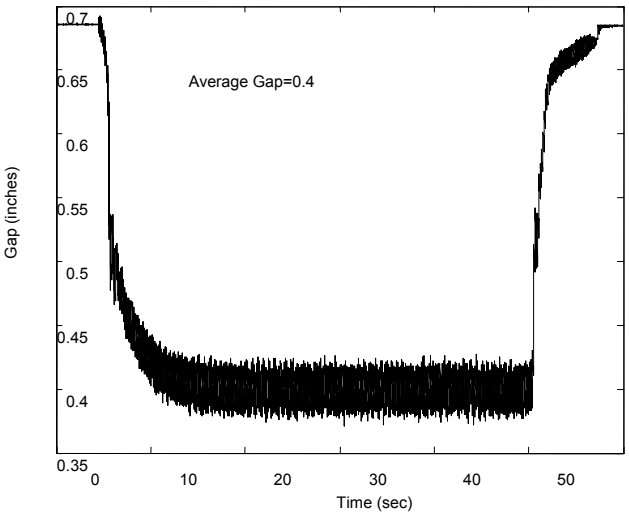

Figure 12: Typical Test Rig Levitation Using PID Control

5 CONCLUSIONS

This paper has presented simple analysis to explore the stability of maglev systems with structural flexibility. Although not discussed exhaustively in this paper, the results can be extended to more complex flexible systems. Initial results with a single degree of freedom test rig corroborate the analytical results. The main conclusion is that PD control can always stabilize a flexible maglev system providing that actuators and sensors are collocated, although the predicted range of stable gains is more limited than in the case of strictly rigid structures.

REFERENCES

Limbert .A., Richardson, H.H. & Wormley, D.N. 1976. Controlled Dynamic Characteristics of Ferromagnetic Vehicle Suspension Providing Simultaneous Lift and Guidance. *Journal of Dynamics Systems, Measurement, and Control* 101: 217-222

Sinha P.K. 1986. *Electrodynamic suspension: Dynamics and Control*, IEEE Control Engineering Series 30.

Goodall R M. 1985. The theory of electromagnetic levitation. *Physics in Technology* 16(5): 207-213

Friedland B. 1986. *Control System Design*, McGraw Hill.

Joshi S.M. 1989. *Control of Large Flexible Space Structures,* Springer Verlag.

West-Vukovich G.S. & E.J. Davison. 1984. The Decentralized Control of Large Flexible Space Structures, *IEEE. Automatic Control*. 29(10): 866-879.

Ogata, K. 1970. *Modern Control Engineering.* Prentice-Hall.

Davey, K., Morris, T., Britcher, C., Tola, R. & McCune, M.. 2001. The Old Dominion University/American Maglev Demonstration System. *6th International Symposium on Magnetic Suspension Technology,* Turin, Italy.